Original Article

http://dx.doi.org/10.3348/kjr.2011.12.6.693
pISSN 1229-6929 · eISSN 2005-8330
Korean J Radiol 2011;12(6):693-699

Korean Journal of Radiology
KJR

Hepatocellular Carcinomas Smaller Than 4 cm Supplied by the Intercostal Artery: Can We Predict Which Intercostal Artery Supplies the Tumor?

Saebeom Hur, MD, Hyo-Cheol Kim, MD, Jin Wook Chung, MD, Min-Uk Kim, MD, Ji Dae Kim, MD, Gyoung Min Kim, MD, In Joon Lee, MD, Young Il Kim, MD, Hwan Jun Jae, MD, Jae Hyung Park, MD

All authors: Department of Radiology, Seoul National University College of Medicine, Institute of Radiation Medicine, Seoul National University Medical Research Center, and Clinical Research Institute, Seoul National University Hospital, Seoul 110-744, Korea

Objective: To predict which intercostal artery supplies a tumor by examining the spatial relationship between hepatocellular carcinoma (HCC) and the intercostal artery feeding the tumor on transverse computed tomography (CT) images.

Materials and Methods: Between January 2000 and September 2009, 46 intercostal arteries supplying HCCs smaller than 4 cm were noted in 44 patients, and CT scans and angiograms of these patients were retrospectively reviewed. The intercostal artery feeding the tumor was marked on the CT scan showing the center of the tumor. In addition, its spatial relationship with the tumor center was examined. The angle of the tumor location was measured on the transverse CT scan in the clockwise direction from the sagittal line on the virtual circle centered in the right hemithorax. Correlations between the angle of the tumor location and the level of the tumor-feeding intercostal artery were assessed with the Spearman rank coefficient.

Results: Of 46 intercostal arteries feeding HCC, 39 (85%) were the first ones observed from the tumor center in a counterclockwise direction on the transverse CT image containing the tumor center. The level of the tumor-feeding intercostal artery was significantly correlated with the angle of the tumor, as the posteriorly located tumor tends to be supplied by lower intercostal arteries, while the laterally located tumor by upper intercostal arteries (Spearman coefficient = -0.537; $p < 0.001$).

Conclusion: We can predict the tumor feeder with an accuracy of 85% as the first intercostal artery encountered from the tumor center in a counterclockwise direction on a transverse CT image.

Index terms: *Hepatocellular carcinoma; Intercostal artery; Computed tomography; TACE; Chemoembolization*

Received April 17, 2011; accepted after revision June 17, 2011.
This study was supported in part by a grant from the Korea Healthcare technology R&D Projects, Ministry for Health, Welfare & Family Affairs, Republic of Korea (A100655) and by Basic Science Research Program through the National Research Foundation of Korea (NRF) funded by the Ministry of Education, Science and Technology (2010-0010788).

Corresponding author: Hyo-Cheol Kim, MD, Department of Radiology, Seoul National University Hospital, 101 Daehak-ro, Jongno-gu, Seoul 110-744, Korea.
• Tel: (822) 2072-2584 • Fax: (822) 743-6385
• E-mail: angiointervention@gmail.com

INTRODUCTION

Chemoembolization is widely employed as a palliative approach in the management of unresectable hepatocellular carcinomas (HCC) (1-4). When an HCC is advanced or exophytic, various extrahepatic collateral arteries (inferior phrenic artery, omental branch, adrenal artery, intercostal artery, internal mammary artery, renal capsular artery, gastric artery, or lumbar artery) commonly supply the tumor (5-18). HCCs abutting the inferolateral aspect of the diaphragm are frequently supplied by the posterior intercostal arteries (7). Park et al. (8) mentioned that the computed tomography (CT) findings suggestive of a collateral blood supply from the intercostal artery are

adhesion/invasion of the abdominal wall, delineation of the intercostal artery within the intercostal space, or branching, streaky lines coursing from the abdominal wall to a tumor.

The common levels of the intercostal arteries that supply HCC are T8 to T12 (8, 19), and the selective angiography of each intercostal artery is time-consuming and tedious. If we can predict which intercostal artery supplies HCCs on CT scan, we can reduce the procedure time and radiation exposure. In this study, we evaluated the spatial relationship between the location of HCCs and the intercostal artery feeding the HCCs on a multi-detector CT scan.

MATERIALS AND METHODS

From January 2000 to September 2009, 21,024 sessions of HCC chemoembolization were performed at our institution in 5372 patients who were referred by physicians for the following reasons: an unresectable tumor, recurrent tumors after curative surgery, or refusal to undergo curative surgery. Most of the angiographic examinations were performed by one of two interventional radiologists (with 16 years experience, or with 27 years experience). Collateral blood supply from the intercostal artery was observed in 177 out of 5372 patients (3%). We excluded 133 patients from the study because the tumor was larger than 4 cm (n = 119) because a large tumor is commonly supplied by multiple intercostal arteries and it is difficult to determine the exact location of the tumor portion supplied by the intercostal artery on CT scan. The arbitrary size of 4 cm was established on the basis of the experience of our institution where more than 2500 sessions of chemoembolization are performed every year; innumerable disseminated tumors (n = 8) because it is impossible to determine which tumor is supplied by the intercostal artery; extrahepatic tumors such as chest wall metastatic deposits supplied by the intercostal artery (n = 3); and CT scans had a section thickness of 5 mm or more (n = 3) (Fig. 1). Therefore, 44 HCC patients (M:F = 40:4; age range, 36-85 years; mean age, 58 years) with 46 HCCs supplied by the intercostal artery were included in this study (Table 1).

The European Association for the Study of the Liver has demonstrated that HCCs can be diagnosed on the basis of coincidental findings of at least two of the following modalities, ultrasound, CT, magnetic resonance imaging, and angiography, which show characteristic features in a focal lesion (20). Of the 44 patients, 22 (50%) were diagnosed as

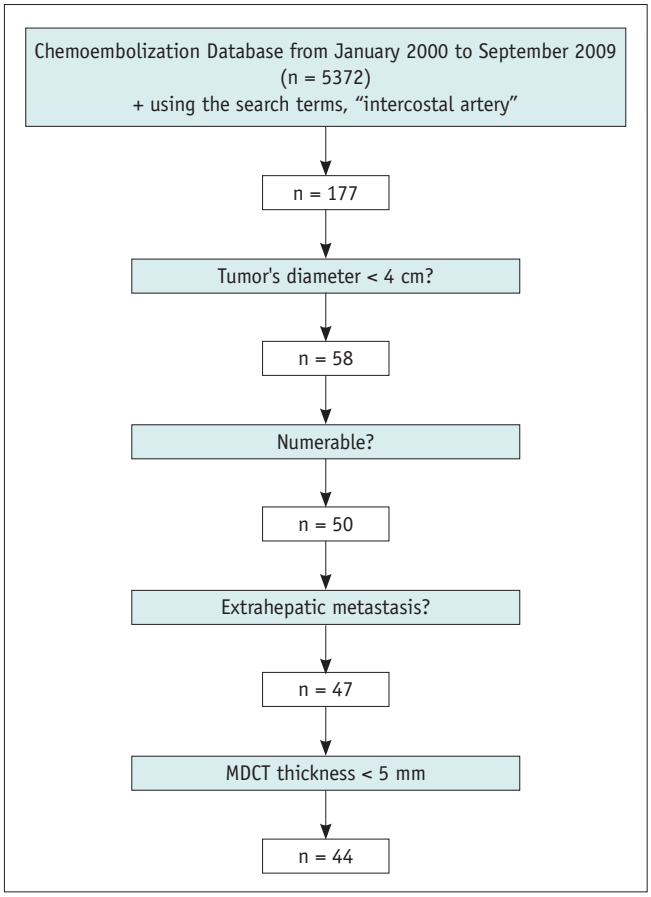

Fig. 1. Flowchart of study population enrollment with exclusion criteria. MDCT = multidetector CT

HCC on the basis of characteristic findings at both dynamic CT and angiography as well as underlying liver cirrhosis. In 22 patients, the histologic diagnosis was obtained with previous surgery (n = 21) or ultrasound-guided needle biopsy (n = 1). This study was approved by our institutional review board, and the need to obtain informed consent was waived because the study was retrospective.

Multi-Detector CT

All patients who underwent chemoembolization at our institution underwent CT before each chemoembolization session and the time interval between CT and chemo-embolization ranged from 1 to 30 days (mean, 17 days).

All CT scans were performed under the full inspiration state. CT was performed with various CT scanners: a four-detector row unit (MX 8000; Philips Medical Systems, Cleveland, OH) (n = 8), an eight-detector row unit (Light Speed Ultra; GE Medical Systems, Milwaukee, WI) (n = 11), a 16-detector row unit (Sensation 16; Siemens, Erlangen, Germany) (n = 13), and a 64-detector row CT unit (Brilliance

Korean Journal of Radiology
KJR

Table 1. Patient and Tumor Characteristics at Baseline

	Number or Median (Interquartile Ranges)
Sex (men/women)	40/4
Age (year)	58 (36-85)
HBs Ag (positive/negative)	32/12
HCV Ab (positive/negative)	9/35
Serum albumin (g/dL)	3.7 (3.3-4.1)
Total bilirubin (mg/dL)	1 (0.8-1.6)
Prothrombin time (%)	79 (71-91)
Ascites (present/absent)	11/33
Serum AST level (IU/L)	44 (29-64)
Serum ALT level (IU/L)	40 (21-66)
Platelet count (x 10^9/L)	117 (64-161)
Serum α-fetoprotein (ng/mL)	266 (24-970)
Child-Pugh class (A/B)	31/13
Tumor size	2.7 (1.1-3.9)
Portal vein thrombosis (present/absent)	5/39
Number of previous chemoembolization session	8.6 (1-21)

Note.— ALT = alanine aminotransferase, AST = aspartate aminotransferase, HBsAg = hepatitis B virus surface antigen, HCV Ab = hepatitis C virus antibody

64; Philips Medical Systems) (n = 12).

The respective scanning parameters used for the 4-, 8-, 16-, and 64-detector row CT scanners were as follows: detector configurations, 4 x 2.5, 8 x 1.25, 16 x 0.75, and 64 x 0.625 mm; section thicknesses, 3.2, 2.5, 3, and 3 mm; reconstruction intervals, 3, 2.5, 3, and 2 mm; and table speeds, 12.5, 13.5, 24, and 46 mm per rotation.

Unenhanced images were first obtained in a craniocaudal direction. The dynamic images consisted of three phases (i.e., hepatic arterial, portal venous, and equilibrium phases). After acquiring unenhanced liver images, contrast medium (iopromide [Ultravist 370; Schering, Berlin, Germany]) was administered, followed by a 30-mL sterile saline flush with a power injector (Multilevel CT; Medrad, Pittsburgh, PA). Contrast medium and saline solution were injected at 3 mL/sec through an 18-gauge plastic intravenous catheter placed in an antecubital vein. Contrast medium volumes varied from 100 to 120 mL. Hepatic arterial phase scan were performed 11-17 seconds after the descending aorta enhancement to 100 HU, as measured by a bolus-tracking technique. The duration of portal venous phase interscan delays were 20-30 seconds. The equilibrium phase images were acquired 180 seconds after completion of contrast medium administration.

Study Definitions

The CT scans and digital subtraction angiograms of these 44 patients were retrospectively reviewed by consensus between two interventional radiologists, (with 2 years of experience and with 5 years of experience). All measurements were performed at a commercially available workstation (XW6200; Hewlett-Packard, CA) with the PACS software (Maroview 5.4; Infinitt, Seoul, Korea). The level of the tumor feeding intercostal artery was determined on angiogram. Tumor size was defined as the largest diameter on transverse CT scans, where the bisecting point of the diameter was designated as the center of the tumor objectively. We devised a systematic method to draw a virtual circle to help analyze the spatial relationship between a tumor and a tumor-feeding intercostal artery more accurately and objectively. The center of the virtual circle was designated on the CT transverse scan showing the center of the tumor by drawing perpendicular bisectors three times, which was concentric with the right hemithorax (Fig. 2A).

Relative Spatial Relationship between a Tumor and a Tumor-Feeding Intercostal Artery on a Transverse CT Image

Because the intercostal artery was seen as an enhancing dot just below the rib, the intercostal artery feeding the tumor was marked on the CT scan showing the center of the tumor. The relative location of the tumor feeding the intercostal artery from the tumor center was determined as the direction (clockwise or counterclockwise) and the order of the intercostal arteries (1st, 2nd, and so on).

Correlation between the Location of a Tumor and the Level of the Tumor-Feeding Intercostal Artery

The location of the tumor was described at an angle which was measured from the sagittal line to the radial line passing the center of the tumor in the clockwise direction on the virtual circle (Fig. 2B).

Correlations between the angle of the tumor location and the level of the tumor-feeding intercostal artery were assessed by the Spearman rank coefficient. A value of $p < 0.05$ was considered to indicate statistical significance. Statistical analyses were conducted using commercially available software (SPSS 12.0 for Windows; SPSS, Chicago, IL).

Fig. 2. 68-year-old man with hepatocellular carcinoma who underwent 8 chemoembolization sessions.
A. Transverse CT scan in hepatic arterial phase shows small hypervascular tumor (star). Center of virtual circle was drawn using following steps: 1) select CT transverse scan showing center of tumor, 2) horizontal line (-) inscribing posterior margin of thorax is drawn, 3) line is bisected by perpendicular line (=), which is again perpendicularly bisected by another horizontal line (≡); mid-point of line (≡) is defined as center of circle (arrowhead), concentric with hemithorax. **B.** Radial line passing through tumor center is drawn and its angle from sagittal line is measured as angle of tumor location (197 degrees in this case). Note 11th intercostal artery (arrow) below 11th rib. **C.** Selective angiography of 11th intercostal artery showing tumor staining (arrow) supplied by tumor feeder (arrowhead).

Table 2. Angle of Tumor Location Supplied by Intercostal Artery according to Level of Intercostal Artery

Level	Incidence (n)	Range (95% CI)	Mean
T8	1	267	267.0
T9	7	240-303 (250-295)	272.3
T10	23	188-265 (216-236)	226.2
T11	12	197-248 (208-227)	217.8
T12	3	194-244	214.7

Note.— CI = confidence interval

RESULTS

Tumor staining supplied by the intercostal artery was detected during the first to the 21st (mean, 8.6 sessions; median, 8 sessions) chemoembolization session. Tumor sizes (maximum diameter) ranged from 11 to 39 mm (average 27 mm). The level of the intercostal artery that supplied the HCC was: T8 (n = 1), T9 (n = 7) (Fig. 3C), T10 (n = 23), T11 (n = 12) (Fig. 2C), and T12 (n = 3) (Table 2).

Relative Spatial Relationship between a Tumor and a Tumor-Feeding Intercostal Artery on a Transverse CT Image

Of the 46 intercostal arteries feeding HCC, 39 (85%) were the first intercostal arteries observed from the tumor center in a counterclockwise direction on the transverse CT image showing the center of the tumor (Fig. 2B), while, 7 (15%) intercostal arteries were not. Five (11%) intercostal arteries feeding HCCs were the first intercostal arteries observed from the center of the tumor in a clockwise direction (Fig. 3). Two (4%) intercostal arteries feeding HCCs were the second intercostal arteries observed from the center of the tumor in a counterclockwise direction.

Correlation between the Location of a Tumor and the Level of Tumor-Feeding Intercostal Artery

The angle of the tumor location ranged from 188 degrees (6 o'clock) to 303 degrees (10 o'clock) in the subcapsular region of the liver. The level of the tumor-feeding intercostal artery was significantly correlated with the angle of tumor location (Spearman coefficient = -0.537; $p < 0.001$). Whereas T11 and T12 intercostal arteries commonly supplied HCC located in the posterior portion of the liver (the angle of tumor location: from 194 to 248 degrees), T9 intercostal artery frequently supplied HCC located in the lateral portion of the liver (the angle of tumor location: from 240 to 303 degrees) (Table 2).

DISCUSSION

The collateral blood supply from the intercostal artery is suspected based on the CT findings of a posterior subcapsular location of a tumor, multiple sessions of previous chemoembolization, and adhesion/invasion of the abdominal wall with the angiographic findings of missing tumor staining observed on CT (8). Though these circumstances prompt the search for an extrahepatic collateral supply, selective angiography of the intercostal artery is relatively difficult and time-consuming due to its small size and multiplicity, which can increase the

Korean Journal of Radiology
KJR

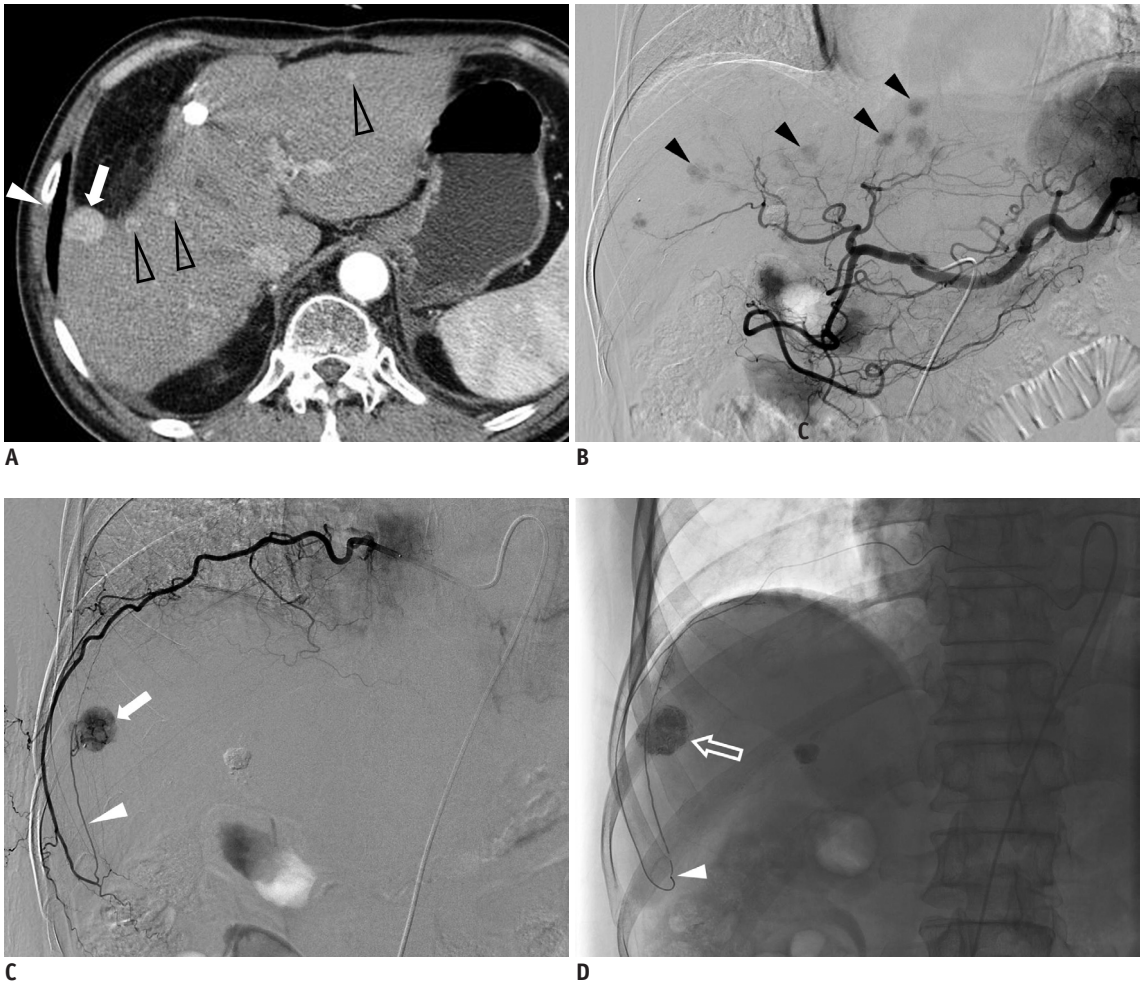

Fig. 3. 61-year-old man with hepatocellular carcinoma who underwent 7 chemoembolization sessions.
A. Transverse CT scan in hepatic arterial phase showing multiple small hypervascular tumors (arrow and open arrowheads). Note 9th intercostal artery below 9th rib. **B.** Celiac angiography performed during 8th chemoembolization session shows multiple small hypervascular tumor stainings (arrowheads) in liver. Tumor indicated by arrow in **A** is not evident on this celiac angiogram. **C.** Selective angiography of 9th intercostal artery shows tumor staining (arrow) supplied by tumor feeder (arrowhead), which makes sharp upward turn at costochondral junction. **D.** Spot image obtained during chemoembolization shows compact retention of iodized oil within tumor (arrow) and microcatheter tip (arrowhead) within tumor feeder.

complication rate, the amount of contrast media, and the dose of radiation. If we can predict the tumor feeding intercostal artery and obtain a spherical tumor staining corresponding to the finding of transverse CT image in the first selective intercostal arterial angiography, the chemoembolization might be performed immediately and further search for tumor feeding intercostal arteries would not be an obligation but an option to take depending on the patient's condition and feasibility of intercostal arterial selection. In this manner, we think reduction of the procedure time, usage of contrast media, and radiation dose is possible. The reduction of contrast media usage might be especially important when the patient has decreased renal function. However, tumor feeders of the intercostal arteries were visualized on the CT scans in only 57% of patients with tumor staining supplied by the intercostal artery, even in the multi-detector CT era (21). Thus, there is a need for better CT features that can predict the level of the intercostal artery supplying a tumor.

Tumor feeders of the intercostal artery always pass the insertion site of the diaphragm to the thoracic cage and supply HCC abutting the diaphragm, making a sharp upward turn near the costochondral junction (8). Because the angle of the upward course of the feeder is steeper than that of the original intercostal artery, a tumor supplied by the intercostal artery tends to be anterior (in a clockwise direction) to the parent intercostal artery on the transverse CT scan showing the center of the tumor. In our study, 85% of intercostal arteries were the first intercostal arteries observed from the tumor center in a counterclockwise

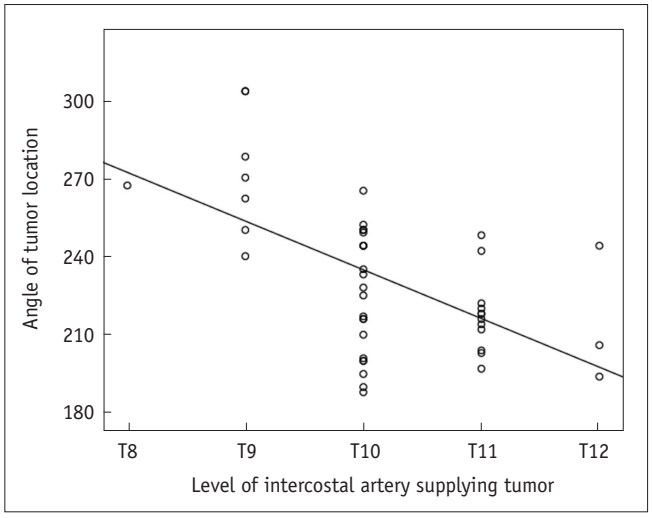

Fig. 4. Relationship between angle of tumor location and level of intercostal artery supplying tumor.

direction on the transverse CT scan. The spatial relationship between the tumor in the liver and the intercostal arteries in the thoracic wall can vary greatly depending on the state of breath; however, this can be considered relatively constant in this study because all CT scans were performed in the full inspiration state.

Although the angle of tumor location and the level of intercostal artery supplying a tumor showed a statistically significant correlation, its clinical impact might be trivial because the range of the angle of tumor location significantly overlapped between the levels of intercostal arteries supplying tumors. However, T9 intercostal arteries are not likely to supply a tumor whose angular location is less than 240 degrees, whereas T11 or T12 intercostal arteries are not likely to supply a tumor whose angular location is greater than 240 degrees (Fig. 4) (Table 2).

Some limitations of the present study require consideration. First, this study was not prospective, and we performed intercostal angiography only in patients suspected of having a blood supply from the intercostal artery to a tumor. Thus, this study probably has a selection bias. Second, various multi-detector CT scanners and scanning parameters were used. Third, the study was performed only in tumors smaller than 4 cm. However, the findings of this study, i.e., the first intercostal artery observed from the tumor center in a counterclockwise direction on the transverse CT scan is the most probable intercostal artery supplying the tumor, can be applied to tumors larger than 4 cm. Fourth, the findings on the CT scans and digital subtraction angiograms were interpreted by the same radiologists. Fifth, the application of the result from this study should be limited to CT examinations performed at the full-inspiration state. During expiration, intercostal arteries go down with the accompanying ribs, while liver tumors rise with the elevating diaphragm and consequently the distance between the intercostal artery and the tumor in the z-axis increases. Thus, a spatial correlation between them at full-expiration should be changed from that at the full-inspiration state.

In conclusion, the first intercostal artery observed from the tumor center in a counterclockwise direction on the transverse CT scan is the most probable one supplying the tumor, with an accuracy of 85% if the intercostal artery supply to the small tumors (smaller than 4 cm) is suspected. Thus, when a HCC is encountered in the right posterior or lateral subcapsular area after multiple sessions of chemoembolization, and the tumor staining is defective or missing on celiac and right inferior phrenic angiography, selective angiography should be performed on the first intercostal artery observed from the tumor center in a counterclockwise direction.

REFERENCES

1. Llovet JM, Bruix J. Systematic review of randomized trials for unresectable hepatocellular carcinoma: Chemoembolization improves survival. *Hepatology* 2003;37:429-442
2. Shin SW. The current practice of transarterial chemoembolization for the treatment of hepatocellular carcinoma. *Korean J Radiol* 2009;10:425-434
3. Lammer J, Malagari K, Vogl T, Pilleul F, Denys A, Watkinson A, et al. Prospective randomized study of doxorubicin-eluting-bead embolization in the treatment of hepatocellular carcinoma: results of the PRECISION V study. *Cardiovasc Intervent Radiol* 2010;33:41-52
4. Ji SK, Cho YK, Ahn YS, Kim MY, Park YO, Kim JK, et al. Multivariate analysis of the predictors of survival for patients with hepatocellular carcinoma undergoing transarterial chemoembolization: focusing on superselective chemoembolization. *Korean J Radiol* 2008;9:534-540
5. Chung JW, Park JH, Han JK, Choi BI, Kim TK, Han MC. Transcatheter oily chemoembolization of the inferior phrenic artery in hepatocellular carcinoma: the safety and potential therapeutic role. *J Vasc Interv Radiol* 1998;9:495-500
6. Miyayama S, Matsui O, Nishida H, Yamamori S, Minami T, Shinmura R, et al. Transcatheter arterial chemoembolization for unresectable hepatocellular carcinoma fed by the cystic artery. *J Vasc Interv Radiol* 2003;14:1155-1161
7. Kim HC, Chung JW, Lee W, Jae HJ, Park JH. Recognizing extrahepatic collateral vessels that supply hepatocellular carcinoma to avoid complications of transcatheter arterial chemoembolization. *Radiographics* 2005;25 Suppl 1:S25-39

8. Park SI, Lee DY, Won JY, Lee JT. Extrahepatic collateral supply of hepatocellular carcinoma by the intercostal arteries. *J Vasc Interv Radiol* 2003;14:461-468
9. Suh SH, Won JY, Lee DY, Lee JT, Lee KH. Chemoembolization of the left inferior phrenic artery in patients with hepatocellular carcinoma: radiographic findings and clinical outcome. *J Vasc Interv Radiol* 2005;16:1741-1745
10. Wang YL, Li MH, Cheng YS, Shi HB, Fan HL. Influential factors and formation of extrahepatic collateral artery in unresectable hepatocellular carcinoma. *World J Gastroenterol* 2005;11:2637-2642
11. Chung JW, Kim HC, Yoon JH, Lee HS, Jae HJ, Lee W, et al. Transcatheter arterial chemoembolization of hepatocellular carcinoma: prevalence and causative factors of extrahepatic collateral arteries in 479 patients. *Korean J Radiol* 2006;7:257-266
12. Kim HC, Chung JW, Jae HJ, Lee W, So YH, Park JH. Hepatocellular carcinoma: transcatheter arterial chemoembolization of the gonadal artery. *J Vasc Interv Radiol* 2006;17:703-709
13. Miyayama S, Matsui O, Taki K, Minami T, Ryu Y, Ito C, et al. Extrahepatic blood supply to hepatocellular carcinoma: angiographic demonstration and transcatheter arterial chemoembolization. *Cardiovasc Intervent Radiol* 2006;29:39-48
14. Kim HC, Chung JW, Choi SH, Jae HJ, Lee W, Park JH. Internal mammary arteries supplying hepatocellular carcinoma: vascular anatomy at digital subtraction angiography in 97 patients. *Radiology* 2007;242:925-932
15. Kim HC, Chung JW, Choi SH, Yoon JH, Lee HS, Jae HJ, et al. Hepatocellular carcinoma with internal mammary artery supply: feasibility and efficacy of transarterial chemoembolization and factors affecting patient prognosis. *J Vasc Interv Radiol* 2007;18:611-619; quiz 620
16. Miyayama S, Yamashiro M, Okuda M, Yoshie Y, Sugimori N, Igarashi S, et al. Hepatocellular carcinoma supplied by the right lumbar artery. *Cardiovasc Intervent Radiol* 2010;33:53-60
17. Miyayama S, Yamashiro M, Okuda M, Yoshie Y, Nakashima Y, Ikeno H, et al. The march of extrahepatic collaterals: analysis of blood supply to hepatocellular carcinoma located in the bare area of the liver after chemoembolization. *Cardiovasc Intervent Radiol* 2010;33:513-522
18. Kim HC, Chung JW, An S, Seong NJ, Son KR, Jae HJ, et al. Transarterial chemoembolization of a colic branch of the superior mesenteric artery in patients with unresectable hepatocellular carcinoma. *J Vasc Interv Radiol* 2011;22:47-54
19. Kim HC, Chung JW, Lee IJ, An S, Seong NJ, Son KR, et al. Intercostal artery supplying hepatocellular carcinoma: demonstration of a tumor feeder by C-arm CT and multidetector row CT. *Cardiovasc Intervent Radiol* 2011;34:87-91
20. Bruix J, Sherman M, Llovet JM, Beaugrand M, Lencioni R, Burroughs AK, et al. Clinical management of hepatocellular carcinoma. Conclusions of the Barcelona-2000 EASL conference. European Association for the Study of the Liver. *J Hepatol* 2001;35:421-430
21. Kim MW, Kim HC, Chung JW, An S, Seong NJ, Jae HJ. Hepatocellular carcinoma: prediction of blood supply from an intercostal artery with multi-detector row CT. *J Vasc Interv Radiol* 2011 [Epub ahead of print]